



**HAL**  
open science

## Investigating the fast spectral diffusion of a quantum emitter in hBN using resonant excitation and photon correlations

Clarisse Fournier, Kenji Watanabe, Takashi Taniguchi, Julien Barjon, Stéphanie Buil, Jean-Pierre Hermier, Aymeric Delteil

► **To cite this version:**

Clarisse Fournier, Kenji Watanabe, Takashi Taniguchi, Julien Barjon, Stéphanie Buil, et al.. Investigating the fast spectral diffusion of a quantum emitter in hBN using resonant excitation and photon correlations. *Physical Review B*, 2023, 107 (19), pp.195304. 10.1103/PhysRevB.107.195304 . hal-04106711

**HAL Id: hal-04106711**

**<https://hal.science/hal-04106711>**

Submitted on 25 May 2023

**HAL** is a multi-disciplinary open access archive for the deposit and dissemination of scientific research documents, whether they are published or not. The documents may come from teaching and research institutions in France or abroad, or from public or private research centers.

L'archive ouverte pluridisciplinaire **HAL**, est destinée au dépôt et à la diffusion de documents scientifiques de niveau recherche, publiés ou non, émanant des établissements d'enseignement et de recherche français ou étrangers, des laboratoires publics ou privés.

## Investigating the fast spectral diffusion of a quantum emitter in hBN using resonant excitation and photon correlations

Clarisse Fournier <sup>1</sup>, Kenji Watanabe <sup>2</sup>, Takashi Taniguchi <sup>3</sup>, Julien Barjon,<sup>1</sup> Stéphanie Buil,<sup>1</sup> Jean-Pierre Hermier,<sup>1</sup> and Aymeric Delteil <sup>1,\*</sup>

<sup>1</sup>Université Paris-Saclay, UVSQ, CNRS, GEMaC, 78000, Versailles, France

<sup>2</sup>Research Center for Functional Materials, National Institute for Materials Science, 1-1 Namiki, Tsukuba 305-0044, Japan

<sup>3</sup>International Center for Materials Nanoarchitectonics, National Institute for Materials Science, 1-1 Namiki, Tsukuba 305-0044, Japan



(Received 9 March 2023; revised 26 April 2023; accepted 10 May 2023; published 25 May 2023)

The ability to identify and characterize homogeneous and inhomogeneous dephasing processes is crucial in solid-state quantum optics. In particular, spectral diffusion leading to line broadening is difficult to evidence when the associated time scale is shorter than the inverse of the photon detection rate. Here, we show that a combination of resonant laser excitation and second-order photon correlations allows us to access such fast dynamics. The resonant laser drive converts spectral diffusion into intensity fluctuations, leaving a signature in the second-order correlation function  $g^{(2)}(\tau)$  of the scattered light that can be characterized using two-photon coincidences, which simultaneously provides the homogeneous dephasing time. We experimentally implement this method to investigate the fast spectral diffusion of a color center generated by an electron beam in the two-dimensional material hexagonal boron nitride. The  $g^{(2)}(\tau)$  function of the quantum emitter measured over more than ten orders of magnitude of delay times, at various laser powers, establishes that the color center experiences spectral diffusion at a characteristic time scale of a few tens of microseconds, while emitting Fourier-limited single photons ( $T_2/2T_1 \sim 1$ ) between spectral jumps.

DOI: [10.1103/PhysRevB.107.195304](https://doi.org/10.1103/PhysRevB.107.195304)

### I. INTRODUCTION

Dephasing processes are ubiquitous in the solid state, often limiting the practical applications of integrated quantum systems. Their characterization, although essential, is often challenging, owing to the great diversity of underlying physical mechanisms and therefore of the amplitude and time scales at which they can affect the system of interest. In the case of single-photon emitters (SPEs), such as color centers in wide gap crystals or self-assembled quantum dots, well-known examples of environment-induced effects acting on the spectral purity include fast dephasing due to phonons [1–4] and spectral diffusion caused by electrostatic fluctuations in the environment [5–9]. The latter effect is typically slower than the emitter lifetime, thus leading to inhomogeneous broadening of the lineshape, and leaving a possibility to expose it by performing spectroscopy faster than its characteristic timescale [10]. However, this method sets highly stringent conditions on the photon detection rate and is limited to slow phenomena. Roundabout methods have been demonstrated, based on photon interferometry [11] or sublinewidth filtering [12,13], but these techniques are in practice limited in terms of either temporal or spectral resolution.

Resonant laser excitation is a powerful way to perform spectroscopy at both high spectral resolution (limited by the laser linewidth) and time resolution (limited by the resolution of the photon counters). For a purely homogeneously broad-

ened two-level system, the photon scattering rate  $C$  is constant and only depends on the laser power and detuning. However, if the emitter experiences spectral fluctuations,  $C$  will inherit these variations as a result of the time-dependent laser-emitter detuning. The induced intensity fluctuations will in turn leave a characteristic signature in the second-order correlation function  $g^{(2)}(\tau)$ , with a short-time bunching that depends on the laser power and detuning relative to the center of the inhomogeneous line shape. In addition,  $g^{(2)}(\tau)$  also provides other essential parameters such as the homogeneous coherence time  $T_2$ , - that can be extracted from the near-zero-delay behavior. By including the influence of spectral diffusion, we show that the Rabi oscillations observed in the  $g^{(2)}(\tau)$  function experience an additional effective damping, which is approximately independent of the spectral diffusion amplitude, but increases with the laser power. Only by accounting for this additional effect can the correct value of  $T_2$  be extracted from the Rabi oscillations. Moreover, contrarily to interferometric techniques [6,11], here detection of resonant photons is not needed and can be performed in phonon sidebands or replica, often available in solid-state quantum emitters.

We implement this approach to study a quantum emitter in the two-dimensional (2D) material hexagonal boron nitride (hBN). This wide-gap material is an attractive platform for quantum photonics in 2D materials due to the high quality of the quantum emitters that it can host [14–16]. Recently, a class of blue-emitting color centers (termed B centers) that can be controllably generated [17–20] have been shown to display bright and stable optical transitions. Their low-temperature linewidth is, however, sizably broader than what is expected

\*aymeric.delteil@usvq.fr

from independent measures of  $T_2$ , which has been found of the order of the excited state lifetime  $T_1$  [21,22]. By measuring photon correlations at various powers and detunings, we here demonstrate that the excess linewidth can be attributed to fast spectral diffusion occurring at a rate of a few tens of kHz. Our results shed new light on the broadening mechanisms of this class of quantum emitters, and our analysis can be applied to other quantum optical systems.

## II. METHODS

### A. Experimental setup and photoluminescence

Our sample consists of a single crystal of high-pressure, high-temperature grown hBN [23] exfoliated on a SiO<sub>2</sub>(285 nm)/Si substrate and subsequently irradiated using an electron beam under 15 kV acceleration voltage [17]. The experimental setup is depicted in Fig. 1(a): the sample is placed on piezoelectric positioners in a 4-K helium closed-cycle cryostat. A confocal microscope based on a 0.8 numerical aperture objective allows to address an individual B center. The SPE is optically pumped using either a nonresonant [405 nm, pulsed or continuous-wave (cw)] or a resonant ( $\sim$ 436 nm, cw) laser. The resonant cw laser is frequency-locked to an external cavity and can be continuously tuned over the relevant wavelength range. Figure 1(b) shows a low-temperature photoluminescence (PL) spectrum of the SPE. The emission features a zero-phonon line (ZPL) and a well-separated ( $\sim$ 160 meV) phonon sideband (PSB). The output port of the confocal microscope includes a dichroic mirror that separates the PSB from the ZPL. Both components are coupled to single-mode fibers and detected by avalanche photodiodes, with the PSB port being the detection channel when resonant excitation is used. The time stability of the ZPL can be observed Fig. 1(c), where no spectral fluctuations exceeding the spectrometer resolution of  $\sim$ 100  $\mu$ eV can be detected. Figure 1(d) shows the fluorescence decay of the emitter under pulsed excitation. An exponential fit provides the lifetime  $T_1 = 1.83$  ns of the excited state.

### B. Resonant excitation of the emitter

The response of the quantum emitter to a resonant laser is shown Fig. 2(a) for various powers. Gaussian fits to the data provide the inhomogeneous linewidth of  $4.0 \pm 0.3$  GHz, well above the natural linewidth (90 MHz) corresponding to the measured  $T_1$  [Fig. 1(d)]. The maximum count rate as a function of the power is shown Fig. 2(b).

We model the B center as a two-level system with a transition energy  $\hbar\omega_{ge}$  fluctuating in time, and following a Gaussian probability density  $\mathcal{G}(\omega_{ge})$  of width  $\Delta\nu = 4.0$  GHz. The homogeneous response is proportional to the excited state population [24]:

$$C(\Omega_R, \omega_L, \omega_{ge}) \propto \rho_{ee} = \frac{1}{2} \frac{\Omega_R^2 T_1 / T_2}{(\omega_{ge} - \omega_L)^2 + T_2^{-2} + \Omega_R^2 T_1 / T_2}, \quad (1)$$

where  $\Omega_R$  is the Rabi frequency and  $\hbar\omega_L$  is the laser energy. This expression allows us to define some important parameters, such as the saturation power—the power at which the population reaches half its maximum at zero detuning—which

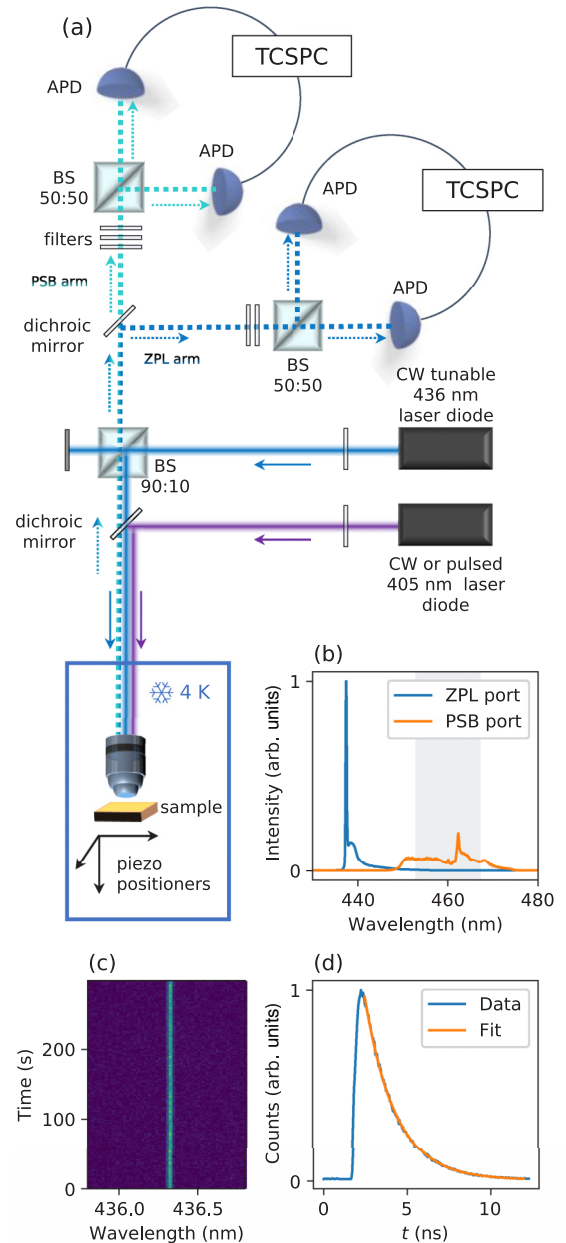


FIG. 1. (a) Experimental setup. (b) PL spectra of SPEs through both output ports. The shaded area denotes the fluorescence filter in the PSB port. (c) PL spectrum as a function of time. (d) PL decay, yielding the emitter lifetime  $T_1 = 1.83$  ns.

corresponds to  $\Omega_R = 1/\sqrt{T_1 T_2}$ . The blue curve on Fig. 2(c) displays the count rate on resonance and in the absence of spectral diffusion, as calculated from Eq. (1). It exhibits the well-known saturation of the two-level system at high power. The blue curve on Fig. 2(d) displays the full width at half maximum (FWHM) of the Lorentzian response described by Eq. (1), which is given by  $2\pi \Delta\nu_{\text{hom}} = 2\sqrt{1 + \Omega_R^2 T_1 T_2 / T_2}$ . The increase of the FWHM when  $P \gtrsim P_{\text{sat}}$  is known as power broadening. In the presence of spectral diffusion, the expected photon emission rate as a function of the laser energy and power can then be numerically computed as the expectation value  $\bar{C}(\Omega_R, \omega_L) = \int d\omega_{ge} \mathcal{G}(\omega_{ge}) C(\Omega_R, \omega_L, \omega_{ge})$ . The

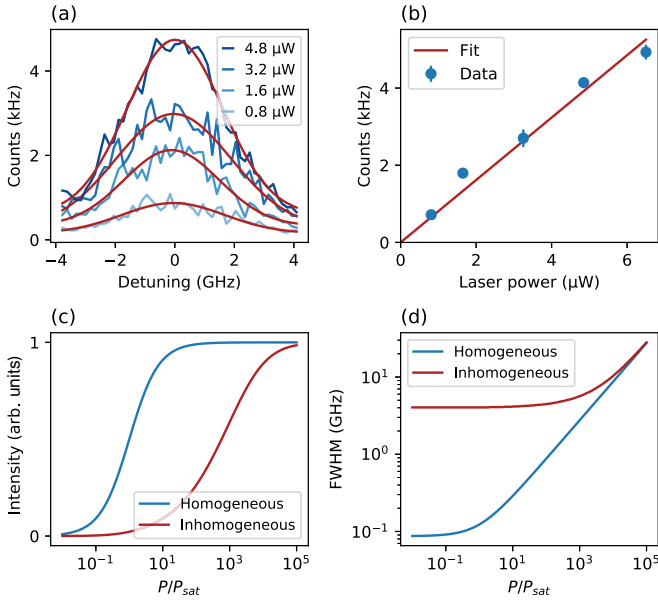


FIG. 2. (a) Resonant laser scans of the SPE. The solid line are Gaussian fits to the data. (b) Maximum count rate as a function of the laser power. (c) Count rate as a function of the saturation parameter  $P/P_{\text{sat}}$ , calculated in the homogeneous (blue line) and inhomogeneous (red line) case. (d) Linewidth of resonant laser scans calculated as a function of  $P/P_{\text{sat}}$  in the homogeneous (blue line) and inhomogeneous (red line) case.

red curve in Fig. 2(c) [respectively 2(d)] displays the calculated count rate (respectively the linewidth) as a function of the saturation parameter  $S = P/P_{\text{sat}} = \Omega_R^2 T_1 T_2$ , for  $T_2 = 2T_1$ . As long as the power-broadened linewidth  $\Delta\nu_{\text{hom}}$  stays below  $\Delta\nu$ , the line shape does not vary much—even above saturation—and the count rate stays approximately linear. Apparent saturation then occurs when the power broadening exceeds the inhomogeneous broadening. This can lead to a potentially large overestimation of the saturation power in such cases, if inferred as the power at which the count rate reaches half its maximum value. In our case, we find  $P_{\text{sat}} \approx 50$  nW from  $T_1$ ,  $T_2$  and  $\Omega_R$  extracted from the experimental data in the following section.

### III. SECOND-ORDER PHOTON CORRELATIONS

#### A. Short-time correlations

In the absence of spectral diffusion, a two-level atom driven by a cw laser exhibits antibunching and, above saturation, undergoes Rabi oscillations, which leave a characteristic signature in the second-order correlation function. At perfect resonance ( $\omega_L = \omega_{ge}$ ), it is described by the following expression [24], accounting for both coherent effects and fast dephasing:

$$g^{(2)}(\tau) = 1 - e^{-\frac{T_1+T_2}{2T_1T_2}\tau} \left( \cos \Omega_R \tau + \frac{T_1 + T_2}{2T_1T_2\Omega_R} \sin \Omega_R \tau \right). \quad (2)$$

This equation is widely used to fit experimental data of coherently driven solid-state quantum emitters [2,21], even in the presence of strong spectral diffusion. In such situation however, the laser-emitter detuning spans a range much

broader than the emitter homogeneous linewidth, so that Eq. 2 is not valid anymore. In the following, we generalize Eq. 2 to include the effect of spectral diffusion.

At a fixed and finite detuning, Eq. 2 is modified by replacing  $\Omega_R$  by  $\sqrt{\Omega_R^2 + \delta^2}$ , where  $\delta = \omega_L - \omega_{ge}$  is the laser-emitter detuning [25], yielding a more general expression of  $g^{(2)}(\tau, \delta)$ . Note that the twofold coincidence rate also depends on  $\delta$  since it varies quadratically with the count rate  $C(\Omega_R, \delta)$  (as defined in Eq. 1).

We now consider the presence of spectral diffusion, with an amplitude much larger than the homogeneous linewidth. If all values of the detuning  $\delta$  are equally likely, each participates to the time-averaged coincidence rate with a relative weight that goes with the squared photon emission rate at this detuning, since  $g^{(2)}$  is measured via two-photon coincidences. Therefore, the experimentally measured, time-averaged,  $\tilde{g}^{(2)}(\tau) = \langle g^{(2)}(\tau, \delta) \rangle_\delta$  can be calculated as the weighted average of  $g^{(2)}(\tau, \delta)$  over all possible detunings, namely:

$$\tilde{g}^{(2)}(\tau) \propto \int d\delta C(\Omega_R, \delta)^2 g^{(2)}(\tau, \delta). \quad (3)$$

This result is independent of the shape and width of the inhomogeneous distribution as long as it exceeds the homogeneous linewidth, *i.e.*,  $\Delta\nu \gg 2\sqrt{1 + \Omega_R^2 T_1 T_2}/T_2$ , which is always the case in the present work. The influence of spectral diffusion on the behavior of  $\tilde{g}^{(2)}(\tau)$  is investigated in detail in the Supplemental Material [26]. It is found not to drastically modify the qualitative behavior of the oscillations, owing to the dependence in  $C(\Omega_R, \delta)^2$  that favors contributions from close-to-zero-detuning components of the integrand. Nonetheless, integration of a continuum of nonresonant components leads to an additional damping of the Rabi oscillations. Therefore, using the zero-detuning Eq. 2 to fit experimental data in a spectrally diffusive situation causes a sizable underestimation of  $T_2$ —especially at high power—and a (slight) overestimation of  $\Omega_R$  by up to 20%. This bias is analyzed in detail in Sec. 3 of the Supplemental Material. It could explain the power-dependent  $T_2$  observed in prior work for quantum emitters experiencing spectral diffusion [21,27,28]. In the intermediate case where  $\Delta\nu \sim 2\sqrt{1 + \Omega_R^2 T_1 T_2}/T_2$ , the exact inhomogeneous distribution has to be accounted for (see Sec. II of the Supplemental Material [26]).

In order to measure the second-order correlation function of the emitter, the PSB output is detected in a Hanbury Brown and Twiss setup. Figure 3 shows  $g^{(2)}(\tau)$  as measured for  $|\tau| < 15$  ns for four different laser powers. At these short delay times, the intensity correlation exhibits the expected behavior, with antibunching as well as damped oscillations. We fit the data with Eq. (3), yielding  $T_2 \sim 2T_1$  at all powers. This indicates that the SPE emits transform-limited photons between spectral jumps. Transform-limited linewidths have been already observed in other families of hBN defects [29,30], although most studies of yellow to infrared color centers concluded to much shorter coherence times [9,31,32]. We emphasize that the use of Eq. (2) instead of Eq. (3) in the fitting procedure yields slightly shorter values of  $T_2$ , ranging from 3.4 ns to 1.8 ns depending on the power. This is further discussed in Sec. IV of the Supplemental Material [26]. Overall, these results provide a good example of a situation where

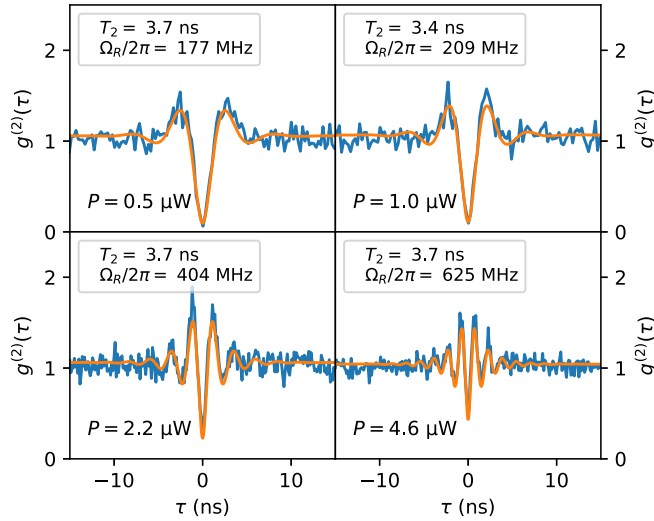


FIG. 3. Blue lines: Short-time correlations at four different laser powers, revealing antibunching and damped Rabi oscillations. Orange lines: Fit to the data using Eq. (3) that accounts for spectral diffusion.

homogeneous properties can be observed in a time-averaged measurement despite a much broader inhomogeneous broadening at large timescales. Other cases where homogeneous properties can be inferred in spite of inhomogeneously broadened energies include spectral hole burning [33], dynamical decoupling [34,35] and mesoscopic ensembles of emitters [36].

### B. Long-time correlations

The longer-time coincidences are processed in logarithmically scaled time bins [37] integrating delay times  $\tau$  up to 10 s. The resulting coincidence rate is normalized by its long-time asymptote. The results for various laser powers, at zero detuning, are shown Fig. 4(a) (solid lines). Photon bunching can be observed at short delays at all powers—albeit with different magnitudes. The amount of bunching decreases with the delay time, reaching a plateau for  $\tau \sim 10$  ms. No other variations in  $g^{(2)}(\tau)$  are visible up to  $\tau = 10$  s. To confirm that the statistics we observe originates from spectral diffusion and not from emitter blinking, we also measure  $g^{(2)}(\tau)$  under non-resonant excitation [red curve in Fig. 4(a)], which features no bunching behavior at all. Incidentally, this confirms the validity of the two-level system approximation for this defect, in contrast to other hBN color centers [16,31,32]. The presence of blinking would yield bunching under both resonant and nonresonant excitation. On the contrary, spectral fluctuations do not turn into intensity fluctuations when the emitter is nonresonantly excited hence exhibits a constant  $g^{(2)}(\tau)$ .

To gain more insight into the dependence of  $g^{(2)}(\tau)$  with the delay time and the laser power, in Fig. 4(b) we plot the degree of bunching  $g^{(2)}(\tau) - 1$  as normalized by its maximum value. We can observe that their time dependence has a similar shape at all powers. However, the inflection point shifts to short times at high power. We define the spectral diffusion timescale  $T_{SD}$  as the time at which the degree of bunching decreases by half its maximum value, *i.e.*,  $g^{(2)}(T_{SD}) - 1 =$

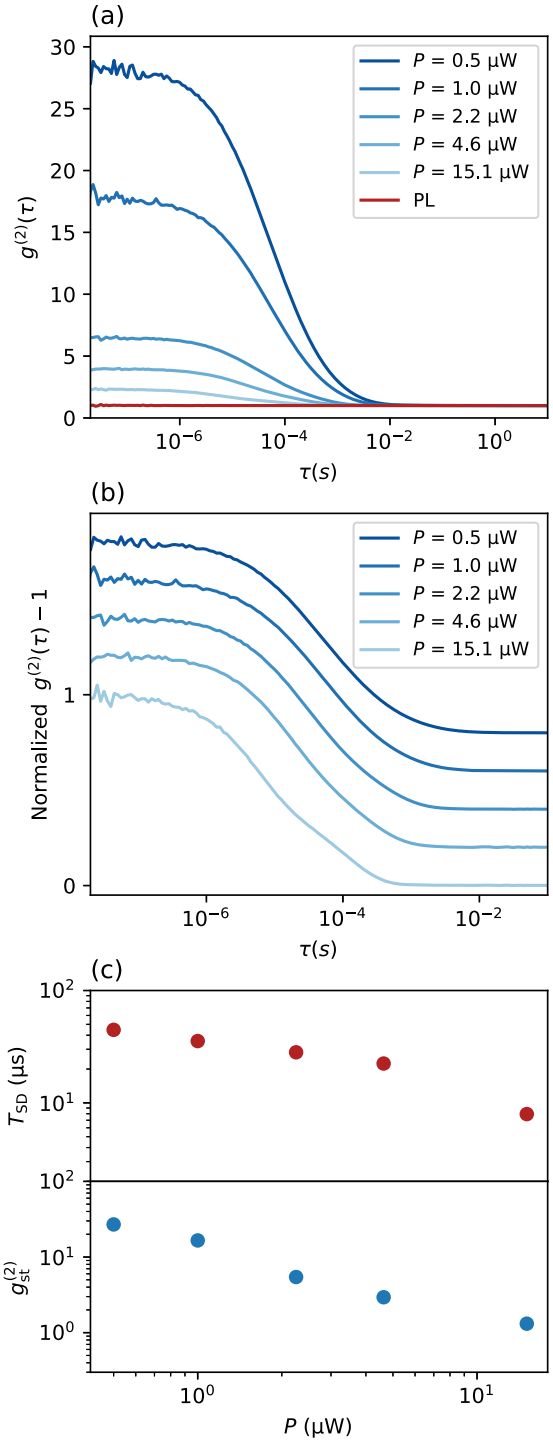


FIG. 4. (a) Long-time  $g^{(2)}(\tau)$  under nonresonant excitation (red line) and under resonant excitation at five different laser powers (blue lines). (b) Same data, but normalized and vertically shifted for clarity. (c)  $T_{SD}$  (upper panel) and  $g_{st}^{(2)}$  (lower panel) as a function of the laser power.

$(g_{st}^{(2)} - 1)/2$ , where we define  $g_{st}^{(2)}$  as the short-time bunching plateau of  $g^{(2)}(\tau)$ . The upper panel of Fig. 4(c) shows  $T_{SD}$  as a function of the laser power.  $T_{SD}$  lies in the 10s of  $\mu$ s range, decreasing with the power from about 50  $\mu$ s down to about 10  $\mu$ s. This time scale is similar to the correlation time

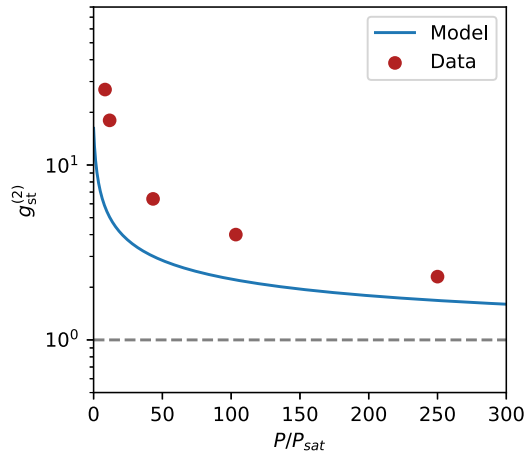


FIG. 5. Solid line:  $g_{st}^{(2)}$  as a function of the laser power, as calculated using Eq. (4). Red dots: Experimental values of  $g_{st}^{(2)}$  as a function of the laser power. Dashed line: High-power asymptote ( $g_{st}^{(2)} = 1$ ).

measured for other families of hBN quantum emitters using interferometric techniques [9,31]. The power dependence of  $T_{SD}$  indicates that the laser has an influence on the spectral diffusion. Moreover, the highest power curve suggests what appears like a splitting into two spectral diffusion processes. Finally, the lower panel of Fig. 4(c) shows the short-time asymptote  $g_{st}^{(2)}$  as a function of the laser power. The amount of bunching strongly decreases with the power [Fig. 4(c), lower panel]. This is due to power broadening decreasing the ratio between homogeneous and inhomogeneous linewidths, as we argue in the following.

To gain more insight into the amount of bunching measured at  $\tau \ll T_{SD}$  and its dependence on the laser power, we calculate the second-order correlation expected in the case of an inhomogeneously broadened two-level system described by Eq. 1. Neglecting the quantum effects occurring at  $\tau \lesssim T_1$ , which have been treated in the previous section, the short-time asymptote  $g_{st}^{(2)}$  can be identified with the classical approximation of  $g^{(2)}(0)$ :

$$g_{st}^{(2)} = \frac{\langle I^2 \rangle}{\langle I \rangle^2} = \frac{\int d\omega_{ge} \mathcal{G}(\omega_{ge}) C(\Omega_R, \omega_L, \omega_{ge})^2}{[\int d\omega_{ge} \mathcal{G}(\omega_{ge}) C(\Omega_R, \omega_L, \omega_{ge})]^2}, \quad (4)$$

Figure 5 shows the result calculated at zero detuning as a function of the laser power (blue curve), for  $T_2 = 2T_1$ . At low power, the value of  $g_{st}^{(2)}$  is fixed by the ratio between the natural linewidth and the width of the inhomogeneous distribution. Intuitively, detection of a photon at time  $t_1$  indicates that  $\omega_{eg} \approx \omega_L$ , which will stay so for an average duration  $T_{SD}$ . Therefore, the probability to detect a second photon at  $t_2$  such

that  $t_2 - t_1 \ll T_{SD}$  is increased as compared to the random  $\omega_{eg}$  case, which therefore generates bunching. At high power on the opposite, the power-broadened homogeneous linewidth exceeds  $\Delta\nu$  such that the intensity fluctuations vanish, which leads to  $g_{st}^{(2)}(P \rightarrow \infty) = 1$ .

The experimental value of  $g_{st}^{(2)}$  is plotted on the same figure (red dots in Fig. 5). The qualitative trend follows the model, however, we observe more bunching than expected from the calculation. The origin of this excess bunching is not understood, and could involve a complex interplay between the transition energy and the laser detuning. Prior work on other semiconductor systems have unveiled various laser-induced spectral jumps mechanisms, which tend to bring the system off-resonant by means of environment modifications [38,39]. Such negative laser-emitter correlations are expected to increase photon bunching. We note that the long integration time ( $>24$  h at the lowest powers) could also have an influence on the spectral diffusion.

#### IV. CONCLUSION

We have shown that photon correlations under resonant excitation constitutes a powerful tool to investigate spectral fluctuations of solid-state quantum emitters, combining high temporal and spectral resolutions. The short-time correlations exhibit a quantum coherent behavior that allows us to extract  $T_2$  and  $\Omega_R$ . The effect of spectral diffusion is accounted for, and results in a faster damping of the Rabi oscillations. On the other hand, the long-time correlations provides information about the spectral diffusion dynamics. We have applied this technique to an individual B center in hBN, showing that it can emit homogeneous ensembles of  $T_{SD}/T_1 \sim 10^4$  consecutive photons that are close to transform-limited ( $T_2/2T_1 \sim 1$ ), before experiencing spectral jumps. This number could be further improved by both reducing the photon lifetime through Purcell effect and reducing the environment noise (with for instance gated devices [30]).

The data generated in this study are available [42].

#### ACKNOWLEDGMENTS

The authors thank A. Pierret and M. Rosticher for flake exfoliation, and S. Roux for sample irradiation. This work is supported by the French Agence Nationale de la Recherche (ANR) under Reference No. ANR-21-CE47-0004-01 (E-SCAPE project). This work also received funding from the European Union's Horizon 2020 research and innovation program under Grant No. 881603 (Graphene Flagship Core 3). K.W. and T.T. acknowledge support from JSPS KAKENHI (Grants No. 19H05790, No. 20H00354 and No. 21H05233).

- [1] G. Cassabois and R. Ferreira, Dephasing processes in a single semiconductor quantum dot, *C. R. Phys.* **9**, 830 (2008).  
 [2] E. B. Flagg, A. Muller, J. W. Robertson, S. Founta, D. G. Deppe, M. Xiao, W. Ma, G. J. Salamo, and C. K. Shih, Resonantly driven coherent oscillations in a solid-state quantum emitter, *Nat. Phys.* **5**, 203 (2009).

- [3] P. Tighineanu, C. L. Dreeßen, C. Flindt, P. Lodahl, and A. S. Sørensen, Phonon Decoherence of Quantum Dots in Photonic Structures: Broadening of the Zero-Phonon Line and the Role of Dimensionality, *Phys. Rev. Lett.* **120**, 257401 (2018).  
 [4] S. White, C. Stewart, A. S. Solntsev, C. Li, M. Toth, M. Kianinia, and I. Aharonovich, Phonon dephasing and

- spectral diffusion of quantum emitters in hexagonal boron nitride, *Optica* **8**, 1153 (2021).
- [5] L. Coolen, P. Spinicelli, and J.-P. Hermier, Emission spectrum and spectral diffusion of a single CdSe/ZnS nanocrystal measured by photon-correlation Fourier spectroscopy, *J. Opt. Soc. A. B.* **26**, 1463 (2009).
- [6] J. Wolters, N. Sadzak, A. W. Schell, T. Schröder, and O. Benson, Measurement of the Ultrafast Spectral Diffusion of the Optical Transition of Nitrogen Vacancy Centers in Nano-Size Diamond Using Correlation Interferometry, *Phys. Rev. Lett.* **110**, 027401 (2013).
- [7] C. Matthiesen, M. J. Stanley, M. Hugues, E. Clarke, and M. Atatüre, Full counting statistics of quantum dot resonance fluorescence, *Sci. Rep.* **4**, 4911 (2014).
- [8] D. Chen, G. R. Lander, K. S. Krowpman, G. S. Solomon, and E. B. Flagg, Characterization of the local charge environment of a single quantum dot via resonance fluorescence, *Phys. Rev. B* **93**, 115307 (2016).
- [9] B. Spokoyny, H. Utzat, H. Moon, G. Grosso, D. Englund, and M. Bawendi, Effect of Spectral Diffusion on the Coherence Properties of a Single Quantum Emitter in Hexagonal Boron Nitride, *J. Phys. Chem. Lett.* **11**, 1330 (2020).
- [10] A. Kuhlmann, J. Houel, A. Ludwig, L. Greuter, D. Reuter, A. D. Wieck, M. Poggio, and R. J. Warburton, Charge noise and spin noise in a semiconductor quantum device, *Nat. Phys.* **9**, 570 (2013).
- [11] X. Brokmann, M. Bawendi, L. Coolen, and J.-P. Hermier, Photon-correlation Fourier spectroscopy, *Opt. Express* **14**, 6333 (2006).
- [12] G. Sallen, A. Tribu, T. Aichele, R. André, L. Besombes, C. Bougerol, M. Richard, S. Tatarenko, K. Kheng, and J.-P. Poizat, Subnanosecond spectral diffusion measurement using photon correlation, *Nat. Photonics* **4**, 696 (2010).
- [13] M. Abbarchi, T. Kuroda, T. Mano, M. Gurioli, and Kazuaki Sakoda, Bunched photon statistics of the spectrally diffusive photoluminescence of single self-assembled GaAs quantum dots, *Phys. Rev. B* **86**, 115330 (2012).
- [14] T. T. Tran, K. Bray, M. J. Ford, M. Toth, and I. Aharonovich, Quantum emission from hexagonal boron nitride monolayers, *Nat. Nanotechnol.* **11**, 37 (2016).
- [15] R. Bourrellier, S. Meuret, A. Tararan, O. Stéphan, M. Kociak, L. H. G. Tizei, and A. Zobelli, Bright UV Single Photon Emission at Point Defects in h-BN, *Nano Lett.* **16**, 4317 (2016).
- [16] L. J. Martínez, T. Pelini, V. Waselowski, J. R. Maze, B. Gil, G. Cassabois, and V. Jacques, Efficient single photon emission from a high-purity hexagonal boron nitride crystal, *Phys. Rev. B* **94**, 121405(R) (2016).
- [17] C. Fournier, A. Plaud, S. Roux, A. Pierret, M. Rosticher, K. Watanabe, T. Taniguchi, S. Buil, X. Quélin, J. Barjon, J.-P. Hermier, and A. Delteil, Position-controlled quantum emitters with reproducible emission wavelength in hexagonal boron nitride, *Nat. Commun.* **12**, 3779 (2021).
- [18] A. Gale, C. Li, Y. Chen, K. Watanabe, T. Taniguchi, I. Aharonovich, and M. Toth, Site-specific fabrication of blue quantum emitters in hexagonal boron nitride, *ACS Photonics* **9**, 2170 (2022).
- [19] B. Shevitski, S. Gilbert, C. T. Chen, C. Kastl, E. S. Barnard, E. Wong, D. F. Ogletree, K. Watanabe, T. Taniguchi, A. Zettl, and S. Aloni, Blue-light-emitting color centers in high-quality hexagonal boron nitride, *Phys. Rev. B* **100**, 155419 (2019).
- [20] S. Roux, C. Fournier, K. Watanabe, T. Taniguchi, J.-P. Hermier, J. Barjon, and A. Delteil, Cathodoluminescence monitoring of quantum emitter activation in hexagonal boron nitride, *Appl. Phys. Lett.* **121**, 184002 (2022).
- [21] J. Horder, S. J. U. White, A. Gale, C. Li, K. Watanabe, T. Taniguchi, M. Kianinia, I. Aharonovich, and M. Toth, Coherence Properties of Electron-Beam-Activated Emitters in Hexagonal Boron Nitride Under Resonant Excitation, *Phys. Rev. Appl.* **18**, 064021 (2022).
- [22] C. Fournier, S. Roux, K. Watanabe, T. Taniguchi, S. Buil, J. Barjon, J.-P. Hermier, and A. Delteil, Two-Photon Interference from a Quantum Emitter in Hexagonal Boron Nitride, *Phys. Rev. Appl.* **19**, L041003 (2023).
- [23] T. Taniguchi and K. Watanabe, Synthesis of high-purity boron nitride single crystals under high pressure by using Ba-BN solvent, *J. Cryst. Growth* **303**, 525 (2007).
- [24] R. Loudon, *The Quantum Theory of Light* (Oxford University Press, Oxford, 2000).
- [25] M. Rezai, J. Wrachtrup, and I. Gerhardt, Detuning dependent Rabi oscillations of a single molecule, *New J. Phys.* **21**, 045005 (2019).
- [26] See Supplemental Material at <http://link.aps.org/supplemental/10.1103/PhysRevB.107.195304> for the details of the calculations and fitting of the Rabi oscillations [21,40,41].
- [27] J. Arjona Martínez, R. A. Parker, K. C. Chen, C. M. Purser, L. Li, C. P. Michaels, A. M. Stramma, R. Debroux, I. B. Harris, M. Hayhurst Appel *et al.*, Photonic Indistinguishability of the Tin-Vacancy Center in Nanostructured Diamond, *Phys. Rev. Lett.* **129**, 173603 (2022).
- [28] J. A. Batalov, C. Zierl, T. Gaebel, P. Neumann, I.-Y. Chan, G. Balasubramanian, P. R. Hemmer, F. Jelezko, and J. Wrachtrup, Temporal Coherence of Photons Emitted by Single Nitrogen-Vacancy Defect Centers in Diamond Using Optical Rabi-Oscillations, *Phys. Rev. Lett.* **100**, 077401 (2008).
- [29] A. Dietrich, M. Bürk, E. S. Steiger, L. Antoniuk, T. T. Tran, M. Nguyen, I. Aharonovich, F. Jelezko, and A. Kubanek, Observation of Fourier transform limited lines in hexagonal boron nitride, *Phys. Rev. B* **98**, 081414 (2018).
- [30] H. Akbari, S. Biswas, P. K. Jha, J. Wong, B. Vest, and H. A. Atwater, Lifetime-Limited and Tunable Quantum Light Emission in h-BN via Electric Field Modulation, *Nano Lett.* **22**, 7798 (2022).
- [31] B. Sontheimer, M. Braun, N. Nikolay, N. Sadzak, I. Aharonovich, O. Benson, Photodynamics of quantum emitters in hexagonal boron nitride revealed by low-temperature spectroscopy, *Phys. Rev. B* **96**, 121202(R) (2017).
- [32] K. Konthasinghe, C. Chakraborty, N. Mathur, L. Qiu, A. Mukherjee, G. D. Fuchs, and A. N. Vamivakas, Rabi oscillations and resonance fluorescence from a single hexagonal boron nitride quantum emitter, *Optica* **6**, 542 (2019).
- [33] P. Palinginis, S. Tavenner, M. Lonergan, and H. Wang, Spectral hole burning and zero phonon linewidth in semiconductor nanocrystals, *Phys. Rev. B* **67**, 201307(R) (2003).
- [34] I. D. Abella, N. A. Kurnit, and S. R. Hartmann, Photon Echoes, *Phys. Rev.* **141**, 391 (1966).
- [35] D. Press, K. De Greve, P. L. McMahon, T. D. Ladd, B. Friess, C. Schneider, M. Kamp, S. Höfiling, A. Forchel, and Y. Yamamoto, Ultrafast optical spin echo in a single quantum dot, *Nat. Photonics* **4**, 367 (2010).

- [36] A. Delteil, V. Blondot, S. Buil, and J.-P. Hermier, First-order coherence of light emission from inhomogeneously broadened mesoscopic ensembles, *Phys. Rev. B* **106**, 115302 (2022).
- [37] T. A. Laurence, S. Fore, and Thomas Huser, Fast, flexible algorithm for calculating photon correlations, *Opt. Lett.* **31**, 829 (2006).
- [38] M. J. Fernée, T. Plakhotnik, Y. Louyer, B. N. Littleton, C. Potzner, P. Tamarat, P. Mulvaney, and B. Lounis, Spontaneous spectral diffusion in CdSe quantum dots, *J. Phys. Chem. Lett.* **3**, 1716 (2012).
- [39] A. Högele, M. Kroner, C. Latta, M. Claassen, I. Carusotto, C. Bulutay, and A. Imamoglu, Dynamic Nuclear Spin Polarization in the Resonant Laser Excitation of an InGaAs Quantum Dot, *Phys. Rev. Lett.* **108**, 197403 (2012).
- [40] H.-P. Breuer and F. Petruccione, *The Theory of Open Quantum Systems* (Oxford University, New York, 2002).
- [41] C. Gardiner and P. Zoller, *Quantum Noise* (Springer-Verlag, Berlin, 2004).
- [42] <https://doi.org/10.5281/zenodo.7938744>.